SSRG International Journal of Electrical and Electronics Engineering
ISSN: 2348-8379/ https://doi.org/10.14445/23488379/IJEEE-V11I5P114

Volume 11 Issue 5, 150-160, May 2024

Original Article

Electroluminescence Images for Solar Cell Fault Detection Using Deep Learning for Binary and Multiclass Classification

Rawad Ahmed Ibrahim Almashhadani[1,2*], Goh Chin Hock[2], Farah Hani Bt Nordin[1], Hazem N. Abdulrazzak[3]

[1]*Institute of Sustainable Energy (ISE), Universiti Tenaga Nasional, Malaysia.*
[2]*Institute of Power Engineering (IPE), Universiti Tenaga Nasional, Malaysia.*
[3]*Department of Computer Communication Engineering, Al-Rafidain University College, Baghdad, Iraq.*

[*]*Corresponding Author : rawadahmed2000@gmail.com*

Received: 09 March 2024 Revised: 10 April 2024 Accepted: 07 May 2024 Published: 29 May 2024

Abstract *- In this study, an automatic solar defect detection and classification system using deep learning was proposed. This study focuses on solar faults in photovoltaic systems identified through Electroluminescence (EL) images by employing a deep learning framework that utilizes both traditional Convolutional Neural Networks (CNNs) and a pre-trained VGG16 and VGG-19 network for feature extraction. This approach was designed to enhance the accuracy and efficiency of solar defect classification. The framework is structured into three main phases: image preprocessing, feature extraction using CNNs, Histogram of Oriented Gradients (HOG) and Artificial Neural Networks (ANN), and classification through a Deep Neural Network (DNN). During preprocessing, images are scaled down to uniform dimensions to ensure consistent learning. They adopted two classification strategies: binary classification (defective or non-defective) and multiclass classification; the class names are 0%, 33%, 67%, and 100% (here, % represents the percentage of defectiveness), which represents the defect likelihood. To refine the model's performance, a data augmentation technique has been utilized on the dataset. The effectiveness of the model was evaluated using various metrics, including the precision, recall, F1-score, and accuracy for two and four classes and obtained on, supported by confusion matrices. VGG-19 model outperformed other models and achieved precision, recall, F1-score and accuracy of 90% each for two classes respectively and similarly 94% for four classes. This study compares two classification methods to assess the ability of the deep learning framework to detect and classify solar defect images automatically.*

Keywords *- Electroluminescence, Photovoltaic, Deep Neural Network, Feature extraction, Defect detection, Solar cell.*

1. Introduction

Renewable energy has historically played an important role in meeting the growing power demand while also protecting the environment. Solar farms produce solar energy; hence, it is a rapidly growing technology that offers an eco-friendly power supply. Nevertheless, various solar flaws that develop because of routine operations or environmental factors reduce the effectiveness of solar energy generation. Such detection can be effectively visualized using Electroluminescence (EL) imaging techniques [1]. EL is the electrically determined emission of light from non-crystalline natural materials, which was first observed and widely concentrated during the 1960s. In the late 1980s, significant advancements were made in EL technology. Notably, Kodak introduced a dual-layer light-emitting device in 1987, integrating thin film deposition techniques for low bias voltages and high luminance efficiency. Subsequently, in 1990, a polymer-based LED emerged [2]. From that point forward, there has been increasing interest and research, and colossal advancements have been made in the upgrades of shading range, luminance productivity, and gadget unwavering quality. The developing interest is, to a great extent, roused by the guarantee of the utilization of this innovation in level board shows [3].

As discussed previously, utilizing EL imaging, it is conceivable to envision defects such as splits and inert cell zones to assess the cell quality, general module, and sunlight-based park quality. As machine vision grows rapidly, a picture-based imperfection discovery technique has been utilized for solar cell surface quality control in the assembly industry [4]. Sunlight-based cell surface quality assessment cannot only improve the creation of the sun-oriented cell module but can also increase the lifetime of the sun-powered cell module. Solar cells are primarily divided into monocrystalline and polycrystalline silicon cells based on

their components. Monocrystalline Si solar cells have a uniform foundation surface [5]. To acquire surface deformity attributes, some component extraction strategies are powerful when the image intensity consistency is fulfilled. Current surface deformity discovery strategies based on machine vision can be classified into four categories in terms of surface highlights:

1. Non-finished surface,
2. Rehashed design surface,
3. Homogeneously finished surface, and
4. Non-homogeneously finished surface.

However, using these approaches leads to a quasi-automatic process of defect detection with limited scope. Techniques that involve machine learning using deep learning have gained significant attention because of their automatic learning and detection functionality. Recently, a few studies have been proposed for deep-learning-based (using the CNN model) solar defect detection according to various configurations of CNN; however, there are research problems to solve.

The key challenge of solar cell manufacturing to generate eco-friendly solar energy is the multiple and indeterminate detection of defects on the solar cell surface in the presence of heterogeneous textures and complex backgrounds. The existing methods focus on directly automated feature extraction and detection using CNN-based deep learning models; however, they do not address the challenge of defect detection under complex and heterogeneous textures. Additionally, current CNN models are based on an automated feature extraction process that may not be reliable when considering the variations in solar surface images; hence, it is necessary to optimize the automatic process of feature extraction using CNN. In addition, the two classification methodologies used by existing techniques-two classes and four classes are mostly focused on flaw identification. Using deep learning models, a unique framework for automatic solar cell detection has been proposed, which includes the following contributions:

Images were scaled down by a factor of 255 during the preprocessing stage before being fed to the model. Image augmentation has also been used to scale up and collect balance data.

Convolution layer stacks and collections of pooling layers were used in the CNN feature extraction procedure. As its name suggests, the convolution layer uses convolution to alter the image. This can be compared with a collection of digital filters. The nearby pixels were combined into one pixel using the pooling layer. The pooling layer subsequently reduces the image dimensions. The convolution and pooling layer processes are naturally performed on a two-dimensional plane because the CNN focuses on the image. This is one of CNN's distinctions of CNN from other neural networks. A DNN was introduced to perform sequential learning and classification. The Paper's contributions can be summarized as:

1. A preprocessing to test the challenges of unbalancing datasets using CNN to extract and feature learning
2. Evaluation of different classification methods to detect defective images
3. Prove the transfer learning using VGG16 and VGG19 as the best solution in 2 Classes and 4- Classes

The rest sections of this paper can be organized as follows: Section 2 presents a review of various related methods. Section 3 presents the design of the methodology. Section 4 presents the simulation results and evaluation. Finally, Section 5 presents our conclusions and future work.

2. Related Works

In the past decade, several image-processing-based techniques have been introduced for solar-cell defect detection using semi-automated and automated approaches. Various techniques based on semi-automatic defect detection have been proposed in [6]. The basic direct iterative bunching superpixel strategy proposed in [6] is a method for problem area identification. They exhibited robotizing imperfection recognition in a solar vitality framework utilizing warm imaging to create an exact and opportunistic arrangement of unsafe conditions.

In [7], the authors intended to recognize the types and areas of deformities. Initially, the picture was pre-handled, and the solar cell was partitioned into sub-cuts. At that point, homomorphism and high-pass channels were applied to the sub-cuts to accomplish picture upgrades, which could keep the picture subtleties better while stifling the clamour. The surface deformity recognition technique proposed in [8] is dependent on the Mobile Net-SSD model and is applied to recognize the sorts and areas of surface imperfections. In the preprocessing stage, a local arranging technique was introduced to remove the principal body of the imperfection, diminish excess parameters, and improve the location speed and accuracy.

The information upgrade increased the heartiness of the calculation. The way of thinking of Mobile Net, a lightweight system, is to improve the recognition accuracy, reduce the registration stack, and shorten the preparation time of this calculation. The Mobile Net and SSD were acclimated to distinguish surface imperfections, with the end goal of separating small deformities from the foundation. The Multi-scale Feature Selective Matching (MFSM) fragment disengagement precisely abandons what is proposed in [9]. To feature the separation territory and debilitate the foundation, they utilize the Parameter-Upgraded Climatic Dispersing Model (PASM) to improve picture differentiation and protect disengagement deformity locale data. At that point, the multi-

scale slope highlight was utilized to acquire the multi-scale highlight saliency map, including every imaginable shape from the improved image. The author of [10] created and exhibited a pipeline for the improvement and assessment of programmed cell arrangement calculations based on EL imaging. They gave pertinent rules for improvement throughout the entire procedure and exhibited their application in a praiseworthy case. The author in [11] presented a computational plan for the pseudo-colorization of EL pictures to feature deformity areas in solar cells for human review. They gave a layout EL picture and pseudo-shading names on its deformity districts; they forced the pseudo hues to other greyscale EL pictures concerning diverse imperfection types and picture structures by format highlight grouping and pseudo-shading movement.

The focus pixel angle data proposed in [12] are applied to an inside symmetric neighbourhood double example (CPICS-LBP), which could intertwine the CPICS-LBP by thresholding every pixel of the picture into a paired code. The arrangement of deformities in a heterogeneous foundation can be significantly upgraded. A far-reaching survey of the structure and manufacture of solar cells aided by ML systems was presented in [13]. ML strategies have been demonstrated to be powerful in helping plan and create solar cells when information is appropriately gathered to counterfeit neural systems and hereditary calculation (GA), the two most applied ML procedures, and the themes in the advancement of gadget structures and improvement of manufacturing forms.

The author in [14] presented the discovery and division of breaks in EL pictures of mono- and polycrystalline solar modules. It exhibited a regulated learning procedure that only used picture-level explanations to acquire a technique that was suitable for portioning breaks on EL pictures of solar cells. In [15], a strategy for solar-cell issue identification in EL pictures utilizing SVM and RF was proposed. SVM (RBF bit) and RF were applied to identify the shortcomings of the solar cells. Two area extraction calculations were performed. Those who assessed the pictures sorted and categorized them into four types of flaws: finger disappointment and three types of splits, depending on their seriousness.

As part of the progressive advantages of deep learning technology, deep learning-based automated solar cell defect detection strategies were recently designed [16]. Significant learning is required to identify solar-cell surface defects, as proposed in [16]. To collect the networks underlying loads, Deep Belief Networks (DBN) was first constructed and prepared. An intelligent defect-detection method based on deep learning was proposed in [17]. The method first builds a network based on the sample characteristics. The initial network value is obtained through training. Subsequently, a neural algorithm was used to adjust the system parameters to acquire the mapping connection between the preparation tests and imperfection-free layouts. The author in [18] focused on the first achievable concentration for the identification of deformities in solar cells. They proceeded to remove cells from the perspective of solar module pictures and arrange the cell pictures by utilizing a CNN in a completely mechanized manner. They presented a profoundly put-together characterization pipeline concerning EL pictures. In [19], the authors planned a visual deformity recognition strategy based on a multiphoton profound CNN.

The image information of every solar cell presented in [20] is processed through a progression of image-processing calculations and then placed into an all-around prepared neural system for grouping. Profound learning was utilized to identify defects in Photovoltaic (PV) modules. A convolutional neural system with seven layers was built to characterize faulty battery boards and present a technique wherein a solitary battery cell can be extracted from the EL images of the PV module and in [21] proposed a programmed discovery of such imperfections in the solitary picture of a Photovoltaic (PV) cell. The hardware requirements of these techniques differ from one another and are determined by their unique application contexts.

The more hardware-productive methodology depends on the available highlights that are characterized in a Support Vector Machine (SVM), the more hardware-requesting approach utilizes a start-to-finish profound Convolutional Neural System (CNN) for sudden spikes in demand for an illustration processing unit (GPU). In [22], an imperfection discovery technique that is dependent on a CNN was proposed. Google Net is one of the prime CNN models for vision registration owing to its fewer neurons, limited scope parameters, and multifaceted nature.

In [23], a novel methodology utilizing light Convolutional Neural System (CNN) engineering for the programmed identification of photovoltaic cell surrenders in EL pictures was presented. This methodology achieved the best-in-class results on the first openly accessible solar cell dataset of EL pictures. In [24], ML models built the structure-property relationship and, along these lines, executed the quick screening of OPV materials. They investigated a few articulations for particle structures, that is, pictures, ASCII strings, descriptors, and fingerprints, as contributions to ML calculations.

During the time spent discovering superior materials for Natural Photovoltaics (OPVs), the connection between substance structures and photovoltaic properties could be established even before incorporating them. In [25], a novel use of DCNNs to address PV cell debasement was proposed. The examinations led on the "Photovoltaic Pictures Dataset," a gathered dataset, were introduced to show the debasement issue and completely assess the strategy displayed. Energy problems are ubiquitous and have recently been studied to address them [26-28]. Thus, solar energy efficiency has also

become a challenge. From the above studies, it is noticed that automatic deep learning-based methods have received great attention for effective defect detection; however, so far, very little work has been proposed with a limited scope. This study proposes a scalable and efficient deep-learning model for solar cell defect detection.

3. Methodology

This section presents the design of the methodology. Figure 1 shows the architecture of the proposed system.

3.1. Dataset and Preprocessing

The dataset is publicly available at https://github.com/zae-bayern/elpv-dataset. A total of 2624 EL Photovoltaic (ELPV) images were obtained. In this study, a set of conditional probabilities (0%, 33%, 67%, and 100% defect likelihood) that defined the labels of each solar cell image are utilized.

A sample of the images is shown in Figure 2. An overview of the number of cells in each defect likelihood category is presented in Figure 3 and Table 1. Each pixel in each image was rescaled to 1/255. This rescaled the pixels in the range [0, 1]. Scaling every image to the same range [0, 1] makes the images contribute more evenly to the total loss. Treating all images in the same manner, some images have a high pixel range, whereas others have a low pixel range. The images share the same model, weights, and learning rate as CNN, which delivers improved accuracy.

3.2. Dataset Augmentation

Data augmentation generates more training data from existing training samples by augmenting the samples via several random transformations on images. The goal is for the model to learn different patterns during training. This helps expose the model to more aspects of the data and generalize it better.

Obtained transformed images from the original dataset. It is a technique of applying different transformations to the original images that results in multiple transformed copies of the same image. Each image, however, is different from the others in certain aspects, depending on the augmentation techniques, such as shifting, rotating, flipping, and brightness. In addition, all images were resized to 224×224 for the target size of data augmentation.

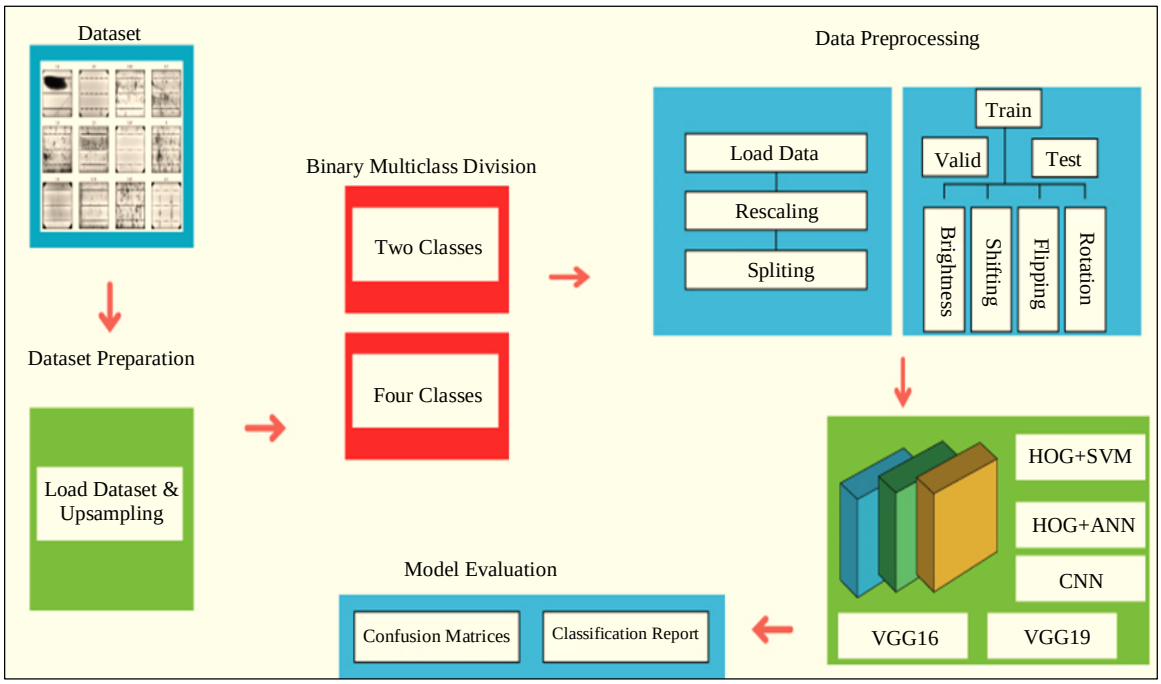

Fig. 1 Methodology used in this study

Table 1. Details of dataset

Defect Classes	No. of Images
0%	1508
33%	295
67%	106
100%	715
Total	2624

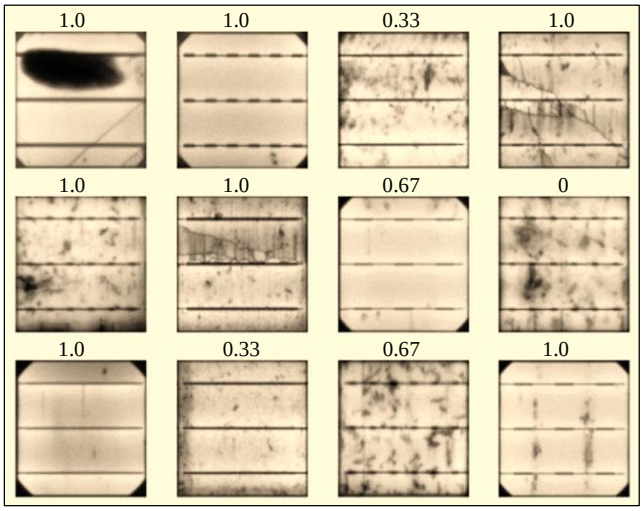

Fig. 2 Sample images of the dataset

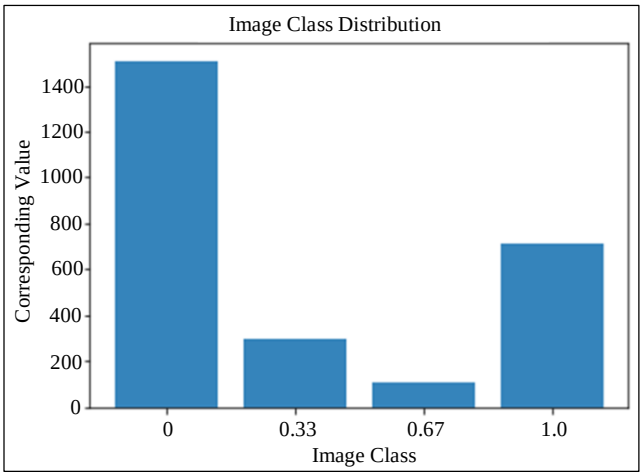

Fig. 3 Bar graph of the details of each category in the dataset

3.3. Upsampling of Classes

In addressing the class imbalance observed within our dataset, a sampling technique has been employed to ensure that each category is equally represented. To augment the number of images across classes, an image data generator has been used. This tool allowed us to artificially enhance our dataset, ensuring that each class reached a balanced distribution [29]. Details of the two-class dataset are listed in Table 2. The details of the four-class balanced dataset are listed in Table 3.

Table 2. Two-class solar cell dataset after up-sampling

Type of Sample	Number of Images
Non-Defected Samples	1508
Defected Samples (0.33, 0.66, 1.0)	1116
Total Samples	**2624**

Table 3. Four-class balanced dataset after up-sampling

Probability	Number of Images
0 Probability	1508
0.33 Probability	1499
0.66 Probability	1426
1.0 Probability	1430
Total Samples	**5863**

3.4. Splitting Training, Validation and Testing data

The training dataset was further divided into validation and testing datasets for the model evaluation. Usually, model training occurs on a training dataset, whereas, because the training set was considered as an exposed dataset, that train set cannot use that exposed dataset for evaluation; therefore, an unseen dataset that has not been used during training of the model. Thus, the dataset was divided our up-sampled dataset into test and training datasets with a ratio of 80:20 percent.

3.5. Model Training

In this step, the model for training was the selected model. The details of the utilized models are as follows:

Creating Descriptor of Histogram of Oriented Gradients (HOG): The HOG is a feature descriptor that is often used to extract features from image data, as shown in Figure 4.

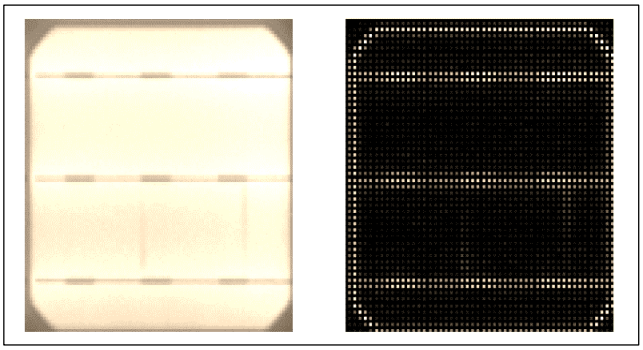

Fig. 4 HOG-based feature-extracted image

Creatin the SVM Model: The features extracted from the HOG techniques are utilized in the SVM model, which is imported from the sklearn library.

Creating ANN Model: In this model, using Keras APIs, four fully connected dense layers were used to create an ANN model. The first layer contains an input layer of 128 units. The second and third layers were hidden layers with 1024 and 512 units, respectively. The last layer is the output layer, which has two or four units with the softmax activation function. The Softmax activation function is used to provide the output from two or four classes. The features extracted from the HOG are also utilized in this model.

Creating the CNN Model: For this model, a convolution layer was used with 32 filters, and the kernel size was 3 × 3. The input shape of the filter was 224×224, and the activation was 'Relu.' Max pooling with a 2x2 kernel size is added after the first convolution layer. Then, 64 filters in the second layer, each with a 3x3 kernel and the activation "Relu." Max pooling with a 2x2 kernel size is added after the second convolution layer. Similar to the second convolution layer, a third convolution layer was added. After flattening, 64 units of dense layer were added, and at the end, two or four units of dense layer were added for classification with the Softmax activation function. The Softmax activation function is used to provide the output from two or four classes.

Using Pre-Trained Models (VGG16 and VGG19): To train a CNN from scratch, a significantly large amount of data is required, and it is not always possible to collect large datasets. However, the need for a large training dataset can be avoided by utilizing pre-trained weights. These two models have different architectures. Moreover, The VGG16 model contains 13 convolutional layers, whereas the VGG19 model contains 16 convolutional layers; along with this, they contain dense and batch normalization layers in their architecture.

The utilization of pre-trained weights also accelerates the learning process by making it more accurate and requires less training data. Therefore, the pre-trained models VGG16 and VGG19 were preferred in this study, and the CNNs used had already been trained on the ImageNet dataset. ImageNet is a large-scale labelled dataset containing more than 14 million images spanning over 20,000 classes. The pre-trained weights, or the weights obtained during training on the ImageNet dataset, were used during training. The pre-trained layers were frozen to apply the transfer-learning technique. Each model included a batch normalization layer before the fully connected layer.

After flattening the model, dense layer 1, which has 128 units with the ReLU activation function, is added to the fully linked layer. After dense layer 1, a batch normalization layer was added. Next, a dropout layer with a dropout size of 0.4 is added. Dense Layer 2, which has 64 units with the activation function "ReLU," is added after the dropout layer. After dense layer 2, a dropout layer with a 0.3 dropout size of added, and dense layer 3, which has two or four units with the Softmax activation function, is added. The Softmax activation function is used to provide the output from two or four classes.

3.6. Model Evaluation

After model training, confusion metrics and classification report parameters have been used to evaluate the models on unseen data. This process is used to test the performance of the trained model.

4. Experimental Analysis

The following experimental criteria were used to conduct the current experiments: the deep learning backend for simulation was either Keras or TensorFlow, and the programming language was Python. On a 12-GB NVIDIA Tesla P40, the model training processes were performed. The outcomes of the proposed model are also compared in this section.

4.1. Comparative Results

Precision, recall, F1-score, and accuracy rate were the metrics used to evaluate the performance. These results were computed using parameters such as True Positive (TP), True Negative (TN), False Positive (FP), and False Negative (FN).

This section presents the comparative results obtained by considering both 2-Class and 4-Class datasets using the different methods discussed above. The confusion matrices of all models for the two classes are shown in Figure 5, and those of all models for the four classes are shown in Figure 6. The parameters extracted from the confusion matrices are listed in Table 4.

$$Precision = \frac{TP}{TP+FP} \quad (1)$$

$$Recall = \frac{TP}{TP+FN} \quad (2)$$

$$Accuracy = \frac{TP+TN}{TP+TN+FP+FN} \quad (3)$$

$$F1-score = \frac{2 \times Precision \times Recall}{Precision + Recall} \quad (4)$$

4.2. Classification Results

HOG + SVM: The results obtained from the HOG + SVM model for two-class classification were in terms of accuracy, recall, precision, and F1-score (74%, 72%, 73%, and 72%, respectively). Accordingly, the sum of true negatives, false negatives, and false positives was high, low, and low, respectively.

Owing to a low sum of false negatives and false positives, one class was found with low evaluation values. Table 4. demonstrates that the overall SVM accuracy for the two classes obtained was 74%. HOG+SVM reported that for the classification of four classes, the accuracy, recall, precision, and F1-score (78%, 77%, 77%, and 76%, respectively).

Table 4. Performance of the utilized models

No. of Classes	Models	Accuracy (%)	Precision (%)	Recall (%)	F1-Score (%)
Two Classes	HOG+SVM	74	73	72	72
	HOG+ANN	77	78	77	76
	CNN	82	82	82	82
	VGG16	89	89	89	89
	VGG19	90	90	90	90
Four Classes	HOG+SVM	78	77	77	76
	HOG+ANN	77	78	77	76
	CNN	85	86	85	86
	VGG16	93	93	93	93
	VGG19	94	94	94	94

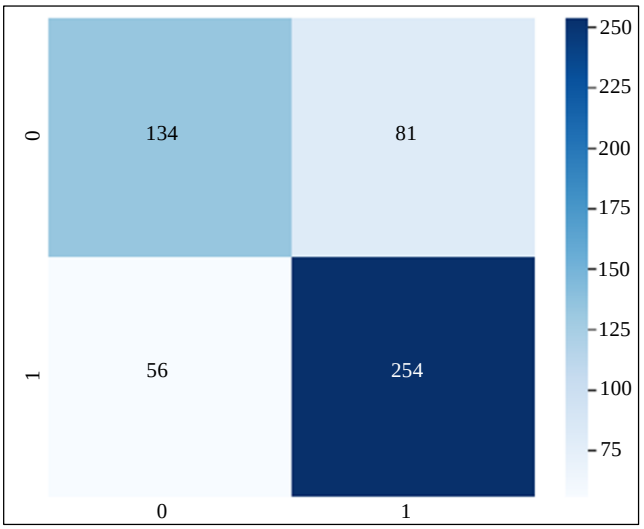

(a)

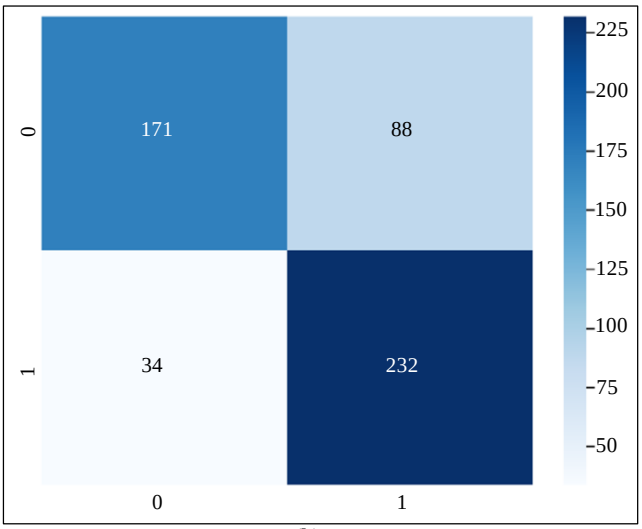

(b)

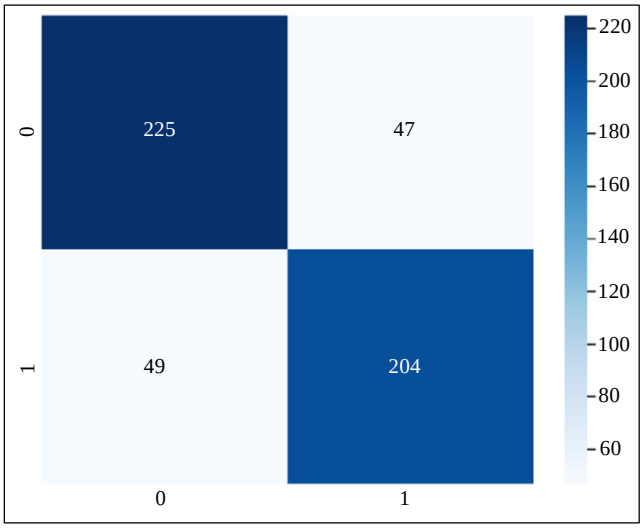

(c)

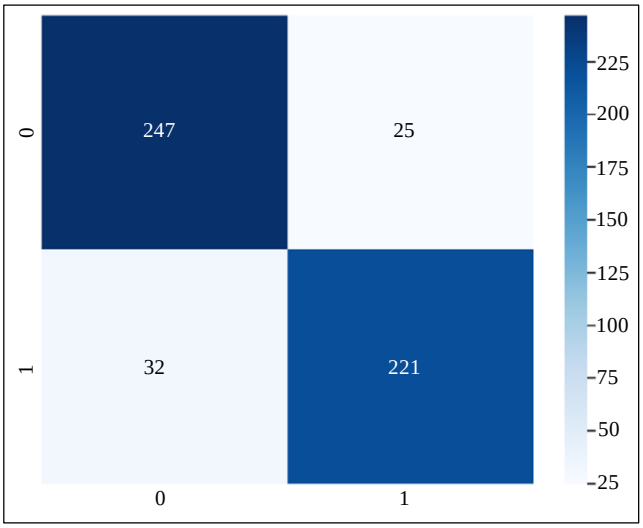

(d)

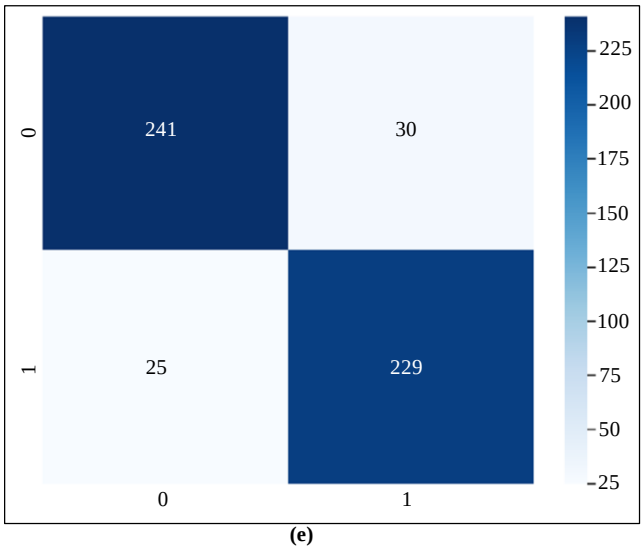

(e)

Fig. 5 Confusion matrices for the two classes on the testing dataset (a) HOG+SVM, (b) HOG+ANN, (c) CNN, (d) VGG16, and (e) VGG19.

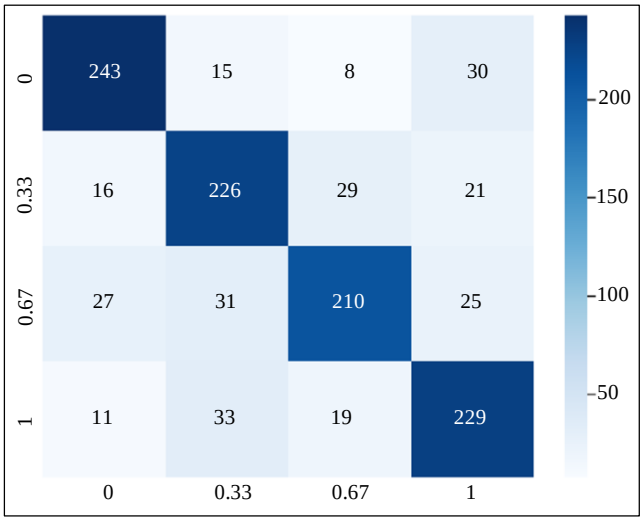

(a)

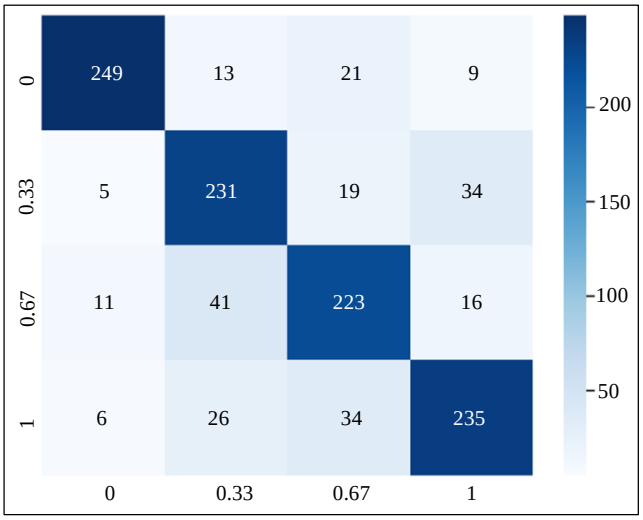

(b)

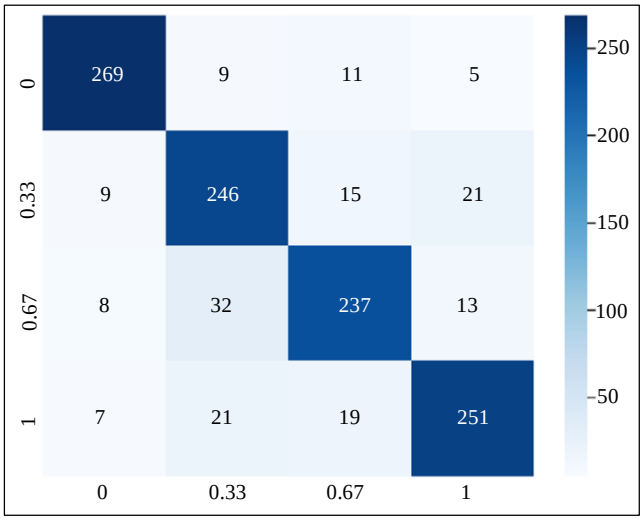

(c)

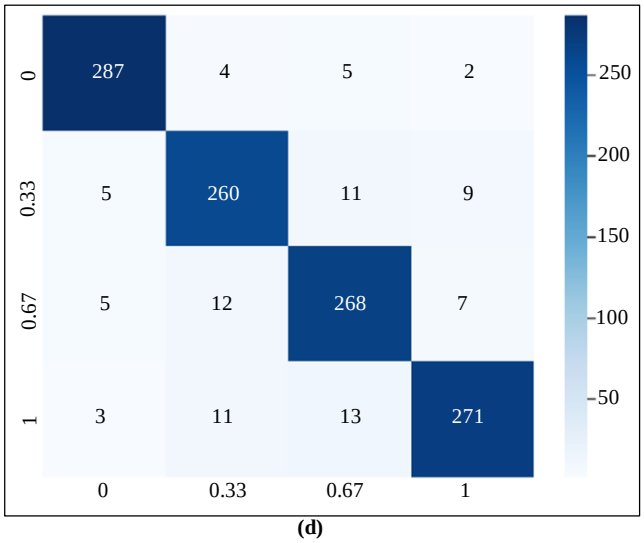

(d)

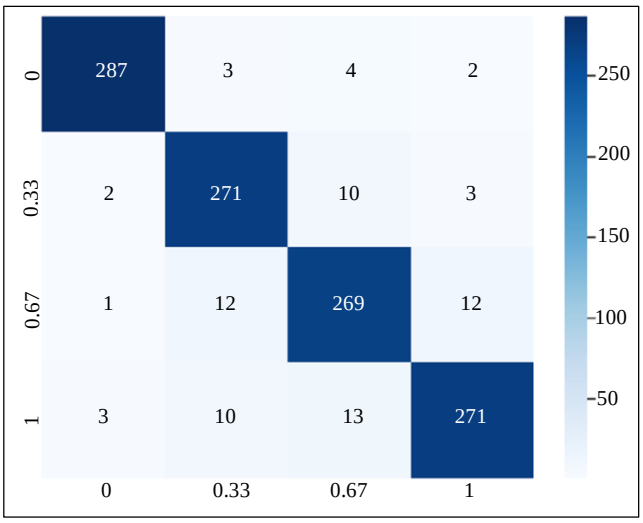

(e)

Fig. 6 Confusion matrices four classes on the testing dataset (a) HOG+SVM, (b) HOG+ANN, (c) CNN, (d) VGG16, and (e) VGG19.

This indicates that the sum of the False Positives, False Negatives, and True Negatives was low, low, and high, respectively. HOG + ANN: For the classification of two classes, ANN showed that the classes were classified with good precision, recall, and F1-score compared with HOG+SVM. The precision value was 78%, which means that the sum of the false positives was low.

For recall, the value was 77% because the sum of false negatives was low. The accuracy of the model for the two classes was 77%, as shown in Table 4, which is better than that of the SVM+HOG model. For the classification of the four classes, HOG+ANN surprisingly achieved 80% precision, recall, F1-score, and accuracy.

CNN: The CNN model's categorization of the two classes shows that the 0 class was separated because its precision, recall, and F1-score reached satisfactory levels (82%, 82%, 81%, and 82%, respectively). This can be explained by the fact that the sum of genuine negatives was large, and the sum of false negatives was low (precision and recall).

The precision and the recall for each class were 82% and 82%, respectively. Additionally, there was a strong specificity and an F1-score of 82% and 82%, respectively. These numbers (precision and recall) can be read as indicating that the total number of false positives and negatives is minimal. The CNN for four classes showed that the zero class was measured with precision, recall, and F1-score (86%, 86%, and 86%, respectively), which means that the sum of false positives was low, the sum of false negatives was low, and the sum of true negatives was high.

VGG16: According to the VGG16 results for the two classes, no class could be identified with high levels of precision, recall, specificity, and F1-score (89%, 89%, 89%, and 89%, respectively). These results were obtained because of the precision and recall of false positive rates and sums of false positives, as well as the high true negative rates. Table 4 shows that the accuracy of the model is 89%. According to the VGG16 results for the four classes, the class was correctly identified with good accuracy, recall, and F1-score (93%, 93%, and 93%, respectively). It was detected rather well at about 0.33 class since the F1-score, accuracy, recall, and specificity were all within acceptable limits. As demonstrated in Table 4, the VGG16's overall accuracy across the four classes was 93%.

VGG19: According to the VGG19 results for the two classes, no class could be identified with high precision, recall, specificity, and F1-score of 90%, 90%, and 90%, respectively. Furthermore, as presented in Table 4, the accuracy of the model was 90%. According to the VGG19 results for the four classes, no class was correctly identified with good accuracy, recall, or F1-score (94%, 94%, and 94%, respectively).

5. Conclusion and Future Work

The performance of the deep learning-based framework proposed for the accurate detection of solar cell defects using EL images is good. The proposed framework consists of different steps, such as preprocessing, feature extraction, classification, and evaluation of models. A preprocessing algorithm is proposed to overcome the challenges of unbalancing the dataset. A CNN architecture is proposed to extract and learn features automatically.

The experimental results show that the proposed module achieves significant improvements in the accuracy, precision, recall, and F1 score. However, transfer learning using VGG16 and VGG19 performed better considering both 2-Classes and 4-Classes. The accuracy of using VGG16 in 2 classes and 4-classes are 89% and 93%, respectively. The VGG19 in 2-

classes and 4- 4-classes accuracy are 90% and 94% respectively.

Funding Statement

This work was supported by UNITEN and Dato' Low Tuck Kwong (DLTK) International Research Grant under the project code 20238023DLTK.

Author Contributions

Rawad Ahmed Ibrahim Almashhadani: Conceptualization, methodology, formal analysis, writing - original draft, Goh Chin Hock; supervision, resources, project administration, Farah Hani Bt Nordin; project administration, validation, Hazem N. Abdulrazzak: proofreading, reviewing and editing the draft copy.

References

[1] F. Spertino et al., "A Power and Energy Procedure in Operating Photovoltaic Systems to Quantify the Losses According to the Causes," *Solar Energy*, vol. 118, pp. 313-326, 2015. [CrossRef] [Google Scholar] [Publisher Link]

[2] Irene Berardone, Juan Lopez Garcia, and Marco Paggi, "Quantitative Analysis of Electroluminescence and Infrared Thermal Images for Aged Monocrystalline Silicon Photovoltaic Modules," *2017 IEEE 44th Photovoltaic Specialist Conference (PVSC)*, Washington, USA, pp. 402-417, 2017. [CrossRef] [Google Scholar] [Publisher Link]

[3] Takashi Fuyuki et al., "Analytic Findings in the Electroluminescence Characterization of Crystalline Silicon Solar Cells," *Journal of Applied Physics*, vol. 101, no. 2, 2007. [CrossRef] [Google Scholar] [Publisher Link]

[4] Irene Berardone, Mauro Corrado, and Marco Paggi, "A Generalized Electric Model for Mono and Polycrystalline Silicon in the Presence of Cracks and Random Defects," *Energy Procedia*, vol. 55, pp. 22-29, 2014. [CrossRef] [Google Scholar] [Publisher Link]

[5] M. Paggi, M. Corrado, and I. Berardone, "A Global/Local Approach for the Prediction of the Electric Response of Cracked Solar Cells in Photovoltaic Modules under the Action of Mechanical Loads," *Engineering Fracture Mechanics*, vol. 168, pp. 40-57, 2016. [CrossRef] [Google Scholar] [Publisher Link]

[6] Moath Alsafasfeh, Ikhlas Abdel-Qader, and Bradley Bazuin, "Fault Detection in Photovoltaic System Using SLIC and Thermal Images," *2017 8th International Conference on Information Technology (ICIT)*, Amman, Jordan, pp. 672-676, 2017. [CrossRef] [Google Scholar] [Publisher Link]

[7] Mei-Ping Song et al., "Research on Broken Corner and Black Edge Detection of Solar Cell," *2018 International Conference on Machine Learning and Cybernetics (ICMLC)*, Chengdu, China, pp. 80-84, 2018. [CrossRef] [Google Scholar] [Publisher Link]

[8] Yiting Li et al., "Research on a Surface Defect Detection Algorithm Based on MobileNet-SSD," *Applied Sciences*, vol. 8, no. 9, pp. 1-17, 2018. [CrossRef] [Google Scholar] [Publisher Link]

[9] Milan Alt et al., "Electroluminescence Imaging and Automatic Cell Classification in Mass Production of Silicon Solar Cells," *2018 IEEE 7th World Conference on Photovoltaic Energy Conversion (WCPEC) (A Joint Conference of 45th IEEE PVSC, 28th PVSEC & 34th EU PVSEC)*, Waikoloa, USA, pp. 3298-3304, 2018. [CrossRef] [Google Scholar] [Publisher Link]

[10] Haiyong Chen et al., "Robust Dislocation Defects Region Segmentation for Polysilicon Wafer Image with Random Texture Background," *IEEE Access*, vol. 7, pp. 134318-134329, 2019. [CrossRef] [Google Scholar] [Publisher Link]

[11] Keh-Moh Lin et al., "Pseudo Colorization of Electroluminescence Images of Multi-Crystalline Silicon Solar Cells for Defect Inspection," *Modern Physics Letters B*, vol. 33, no. 14n15, 2019. [CrossRef] [Google Scholar] [Publisher Link]

[12] Binyi Su et al., "Classification of Manufacturing Defects in Multicrystalline Solar Cells with Novel Feature Descriptor," *IEEE Transactions on Instrumentation and Measurement*, vol. 68, no. 12, pp. 4675-4688, 2019. [CrossRef] [Google Scholar] [Publisher Link]

[13] Fan Li et al., "Machine Learning (ML)-Assisted Design and Fabrication for Solar Cells," *Energy & Environmental Materials*, vol. 2, no. 4, pp. 280-291, 2019. [CrossRef] [Google Scholar] [Publisher Link]

[14] Martin Mayr et al., "Weakly Supervised Segmentation of Cracks on Solar Cells Using Normalized Lp Norm," *2019 IEEE International Conference on Image Processing (ICIP)*, Taipei, Taiwan, pp. 1885-1889, 2019. [CrossRef] [Google Scholar] [Publisher Link]

[15] Claire Mantel et al., "Machine Learning Prediction of Defect Types for Electroluminescence Images of Photovoltaic Panels," *Applications of Machine Learning*, vol. 11139, 2019. [CrossRef] [Google Scholar] [Publisher Link]

[16] Alireza Saberironaghi, Jing Ren, and Moustafa El-Gindy, "Defect Detection Methods for Industrial Products Using Deep Learning Techniques: A Review," *Algorithms*, vol. 16, no. 2, pp. 1-30, 2023. [CrossRef] [Google Scholar] [Publisher Link]

[17] Binbin Ni et al., "Intelligent Defect Detection Method of Photovoltaic Modules Based on Deep Learning" *Proceedings of the 2018 International Conference on Transportation & Logistics, Information & Communication, Smart City (TLICSC 2018)*, 2018. [CrossRef] [Google Scholar] [Publisher Link]

[18] Alexander Bartler et al., "Automated Detection of Solar Cell Defects with Deep Learning," *2018 26th European Signal Processing Conference (EUSIPCO)*, Rome, Italy, pp. 2035-2039, 2018. [CrossRef] [Google Scholar] [Publisher Link]

[19] Haiyong Chen et al., "Solar Cell Surface Defect Inspection Based on Multispectral Convolutional Neural Network," *Journal of Intelligent Manufacturing*, vol. 31, no. 2, pp. 453-468, 2020. [CrossRef] [Google Scholar] [Publisher Link]

[20] Mingjian Sun et al., "Defect Detection of Photovoltaic Modules Based on Convolutional Neural Network," *Machine Learning and Intelligent Communications*, pp. 122-132, 2018. [CrossRef] [Google Scholar] [Publisher Link]

[21] Sergiu Deitsch et al., "Automatic Classification of Defective Photovoltaic Module Cells in Electroluminescence Images," *Solar Energy*, vol. 185, pp. 455-468, 2019. [CrossRef] [Google Scholar] [Publisher Link]

[22] Binhui Liu, Qiangrong Yang, and Yurong Han, "A Photovoltaic Cell Defect Detection Method Using Electroluminescent and Googlenet," *2019 2nd International Conference on Mechanical Engineering, Industrial Materials and Industrial Electronics (MEIMIE 2019)*, pp. 158-166, 2019. [Google Scholar] [Publisher Link]

[23] M. Waqar Akram et al., "CNN Based Automatic Detection of Photovoltaic Cell Defects in Electroluminescence Images," *Energy*, vol. 189, 2019. [CrossRef] [Google Scholar] [Publisher Link]

[24] Wenbo Sun et al., "Machine Learning-Assisted Molecular Design and Efficiency Prediction for High-Performance Organic Photovoltaic Materials," *Science Advances*, vol. 5, no. 11, 2019. [CrossRef] [Google Scholar] [Publisher Link]

[25] R. Pierdicca et al., "Deep Convolutional Neural Network for Automatic Detection of Damaged Photovoltaic Cells," *The International Archives of the Photogrammetry, Remote Sensing and Spatial Information Sciences*, vol. 42, pp. 893-900, 2018. [CrossRef] [Google Scholar] [Publisher Link]

[26] Hemant B. Mahajan, and Anil Badarla, "Experimental Analysis of Recent Clustering Algorithms for Wireless Sensor Network: Application of IoT Based Smart Precision Farming," *Journal of Advanced Research in Dynamical and Control Systems*, vol. 11, no. 9, pp. 116-125, 2019. [Google Scholar] [Publisher Link]

[27] Hemant B. Mahajan, and Anil Badarla, "Detecting HTTP Vulnerabilities in IoT-Based Precision Farming Connected with Cloud Environment Using Artificial Intelligence," *International Journal of Advanced Science and Technology*, vol. 29, no. 3, pp. 214-226, 2020. [Google Scholar] [Publisher Link]

[28] Ashwini B. Gavali, Megha V. Kadam, and Sarita Patil, "Energy Optimization Using Swarm Intelligence for IoT-Authorized Underwater Wireless Sensor Networks," *Microprocessors and Microsystems*, vol. 93, 2022. [CrossRef] [Google Scholar] [Publisher Link]

[29] Francisco J. Moreno-Barea, José M. Jerez, and Leonardo Franco, "Improving Classification Accuracy Using Data Augmentation on Small Data Sets," *Expert Systems with Applications*, vol. 161, 2020. [CrossRef] [Google Scholar] [Publisher Link]